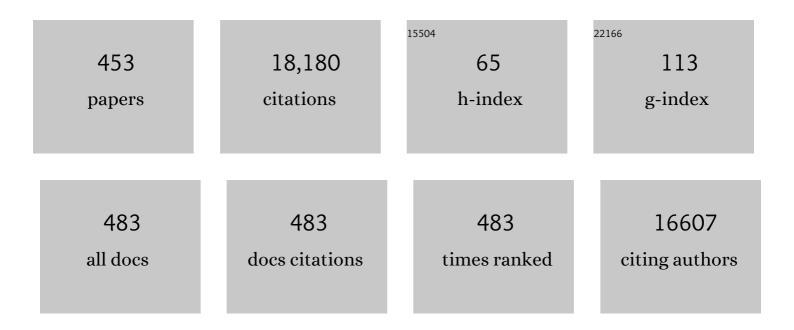
Jin-Ho Choy

List of Publications by Year in descending order

Source: https://exaly.com/author-pdf/4382661/publications.pdf Version: 2024-02-01



Ιινι-Ηο Choy

#	Article	IF	CITATIONS
1	Intercalative Nanohybrids of Nucleoside Monophosphates and DNA in Layered Metal Hydroxide. Journal of the American Chemical Society, 1999, 121, 1399-1400.	13.7	624
2	Inorganic Layered Double Hydroxides as Nonviral Vectors. Angewandte Chemie - International Edition, 2000, 39, 4041-4045.	13.8	576
3	Clay minerals and layered double hydroxides for novel biological applications. Applied Clay Science, 2007, 36, 122-132.	5.2	558
4	Fine Tuning of the Face Orientation of ZnO Crystals to Optimize Their Photocatalytic Activity. Advanced Materials, 2006, 18, 3309-3312.	21.0	552
5	Mesoporous carbon nitrides: synthesis, functionalization, and applications. Chemical Society Reviews, 2017, 46, 72-101.	38.1	534
6	Layered double hydroxide as an efficient drug reservoir for folate derivatives. Biomaterials, 2004, 25, 3059-3064.	11.4	401
7	Soft Solution Route to Directionally Grown ZnO Nanorod Arrays on Si Wafer; Room-Temperature Ultraviolet Laser. Advanced Materials, 2003, 15, 1911-1914.	21.0	285
8	The effect of synthetic conditions on tailoring the size of hydrotalcite particles. Solid State Ionics, 2002, 151, 285-291.	2.7	267
9	Remarkable Capacity Retention of Nanostructured Manganese Oxide upon Cycling as an Electrode Material for Supercapacitor. Journal of Physical Chemistry C, 2009, 113, 6303-6309.	3.1	239
10	Toxicological effects of inorganic nanoparticles on human lung cancer A549 cells. Journal of Inorganic Biochemistry, 2009, 103, 463-471.	3.5	227
11	New Inorganic-Based Drug Delivery System of Indole-3-Acetic Acid-Layered Metal Hydroxide Nanohybrids with Controlled Release Rate. Chemistry of Materials, 2007, 19, 2679-2685.	6.7	225
12	Cellular Uptake Mechanism of an Inorganic Nanovehicle and Its Drug Conjugates:Â Enhanced Efficacy Due To Clathrin-Mediated Endocytosis. Bioconjugate Chemistry, 2006, 17, 1411-1417.	3.6	224
13	Cellular uptake behavior of [γÂ32P] labeled ATP–LDH nanohybrids. Journal of Materials Chemistry, 2001, 11, 1671-1674.	6.7	206
14	Controlled release of donepezil intercalated in smectite clays. International Journal of Pharmaceutics, 2008, 359, 198-204.	5.2	202
15	Layered nanomaterials for green materials. Journal of Materials Chemistry, 2009, 19, 2553.	6.7	198
16	Inorganic Drugâ€Đelivery Nanovehicle Conjugated with Cancer ellâ€Specific Ligand. Advanced Functional Materials, 2009, 19, 1617-1624.	14.9	184
17	Inorganic Metal Hydroxide Nanoparticles for Targeted Cellular Uptake Through Clathrinâ€Mediated Endocytosis. Chemistry - an Asian Journal, 2009, 4, 67-73.	3.3	174
18	Layered double hydroxide nanoparticles as target-specific delivery carriers: uptake mechanism and toxicity. Nanomedicine, 2011, 6, 803-814.	3.3	169

#	Article	IF	CITATIONS
19	Heterostructured Visible-Light-Active Photocatalyst of Chromia-Nanoparticle-Layered Titanate. Advanced Functional Materials, 2007, 17, 307-314.	14.9	165
20	Bio-LDH nanohybrid for gene therapy. Solid State Ionics, 2002, 151, 229-234.	2.7	157
21	Efficient delivery of anticancer drug MTX through MTX-LDH nanohybrid system. Journal of Physics and Chemistry of Solids, 2006, 67, 1024-1027.	4.0	155
22	Relationship between Chemical Bonding Nature and Electrochemical Property of LiMn2O4 Spinel Oxides with Various Particle Sizes:  "Electrochemical Grafting―Concept. Journal of Physical Chemistry B, 1999, 103, 2100-2106.	2.6	137
23	Inorganic delivery vector for intravenous injection. Biomaterials, 2004, 25, 5995-6001.	11.4	135
24	Exfoliation of layered perovskite, KCa2Nb3O10, into colloidal nanosheets by a novel chemical process. Journal of Materials Chemistry, 2001, 11, 1277-1282.	6.7	128
25	Pharmacokinetics, tissue distribution, and excretion of zinc oxide nanoparticles. International Journal of Nanomedicine, 2012, 7, 3081.	6.7	121
26	A novel synthetic route to TiO2-pillared layered titanate with enhanced photocatalytic activity. Journal of Materials Chemistry, 2001, 11, 2232-2234.	6.7	117
27	Biodegradable Inorganic Nanovector: Passive versus Active Tumor Targeting in siRNA Transportation. Angewandte Chemie - International Edition, 2016, 55, 4582-4586.	13.8	117
28	XANES and EXAFS Studies on the Ir-O Bond Covalency in Ionic Iridium Perovskites. Journal of the American Chemical Society, 1995, 117, 8557-8566.	13.7	114
29	Exfoliation and Restacking Route to Anatase-Layered Titanate Nanohybrid with Enhanced Photocatalytic Activity. Chemistry of Materials, 2002, 14, 2486-2491.	6.7	109
30	Mixed valence Zn–Co-layered double hydroxides and their exfoliated nanosheets with electrode functionality. Journal of Materials Chemistry, 2011, 21, 4286.	6.7	109
31	Inorganic–Biomolecular Hybrid Nanomaterials as a Genetic Molecular Code System. Advanced Materials, 2004, 16, 1181-1184.	21.0	106
32	Bifunctional Heterogeneous Catalysts for Selective Epoxidation and Visible Light Driven Photolysis: Nickel Oxide ontaining Porous Nanocomposite. Advanced Materials, 2008, 20, 539-542.	21.0	106
33	Polymer–inorganic supramolecular nanohybrids for red, white, green, and blue applications. Progress in Polymer Science, 2013, 38, 1442-1486.	24.7	105
34	Layered double hydroxide as novel antibacterial drug delivery system. Journal of Physics and Chemistry of Solids, 2010, 71, 685-688.	4.0	102
35	Human-related application and nanotoxicology of inorganic particles: complementary aspects. Journal of Materials Chemistry, 2008, 18, 615-620.	6.7	101
36	Improved electrochromic performances of NiO based thin films by lithium addition: From single layers to devices. Electrochimica Acta, 2012, 74, 46-52.	5.2	100

#	Article	IF	CITATIONS
37	Laponite-based nanohybrid for enhanced solubility and controlled release of itraconazole. International Journal of Pharmaceutics, 2008, 349, 283-290.	5.2	99
38	Intracrystalline Structure of Molecular Mercury Halide Intercalated in High-Tc Superconducting Lattice of Bi2Sr2CaCu2Oy. Journal of the American Chemical Society, 1997, 119, 1624-1633.	13.7	98
39	Itraconazole–Laponite: Kinetics and mechanism of drug release. Applied Clay Science, 2008, 40, 99-107.	5.2	97
40	Phosphate-intercalated Ca–Fe-layered double hydroxides: Crystal structure, bonding character, and release kinetics of phosphate. Journal of Solid State Chemistry, 2011, 184, 171-176.	2.9	97
41	TiO2 thin-films on polymer substrates and their photocatalytic activity. Thin Solid Films, 2006, 495, 266-271.	1.8	95
42	Softâ€Chemical Exfoliation Route to Layered Cobalt Oxide Monolayers and Its Application for Film Deposition and Nanoparticle Synthesis. Chemistry - A European Journal, 2009, 15, 10752-10761.	3.3	95
43	Drug–clay nanohybrids as sustained delivery systems. Applied Clay Science, 2016, 130, 20-32.	5.2	94
44	Mesoporous Iron Oxide-Layered Titanate Nanohybrids: Soft-Chemical Synthesis, Characterization, and Photocatalyst Application. Journal of Physical Chemistry C, 2008, 112, 14853-14862.	3.1	93
45	Anticancer drug encapsulated in inorganic lattice can overcome drug resistance. Journal of Materials Chemistry, 2010, 20, 9463.	6.7	93
46	Cage type mesoporous carbon nitride with large mesopores for CO2 capture. Catalysis Today, 2015, 243, 209-217.	4.4	93
47	Anticancer drug-layered hydroxide nanohybrids as potent cancer chemotherapy agents. Journal of Physics and Chemistry of Solids, 2008, 69, 1528-1532.	4.0	91
48	Microwave Characteristics of BaO-TiO2 Ceramics Prepared via a Citrate Route. Journal of the American Ceramic Society, 1995, 78, 1169-1172.	3.8	90
49	Exfoliation and Reassembling Route to Mesoporous Titania Nanohybrids. Chemistry of Materials, 2006, 18, 1134-1140.	6.7	90
50	Hydrothermal route to ZnO nanocoral reefs and nanofibers. Applied Physics Letters, 2004, 84, 287-289.	3.3	88
51	α-RuCl3/Polymer Nanocomposites: The First Group of Intercalative Nanocomposites with Transition Metal Halides. Journal of the American Chemical Society, 2000, 122, 6629-6640.	13.7	83
52	Macromolecular Nanoplatelet of Aurivillius-type Layered Perovskite Oxide, Bi4Ti3O12. Chemistry of Materials, 2001, 13, 2759-2761.	6.7	83
53	Evolution of Local Structure around Manganese in Layered LiMnO2upon Chemical and Electrochemical Delithiation/Relithiation. Chemistry of Materials, 2000, 12, 1818-1826.	6.7	78
54	Modification of external surface of laponite by silane grafting. Journal of Physics and Chemistry of Solids, 2004, 65, 499-501.	4.0	78

#	Article	IF	CITATIONS
55	Biocompatible Nanoparticles Intercalated with Anticancer Drug for Target Delivery: Pharmacokinetic and Biodistribution Study. Journal of Nanoscience and Nanotechnology, 2010, 10, 2913-2916.	0.9	78
56	LIII-Edge XANES Study on Unusually High Valent Iridium in a Perovskite Lattice. The Journal of Physical Chemistry, 1994, 98, 6258-6262.	2.9	76
57	Emerging nanomaterials with advanced drug delivery functions; focused on methotrexate delivery. Coordination Chemistry Reviews, 2018, 359, 32-51.	18.8	75
58	Review of Clay-Drug Hybrid Materials for Biomedical Applications: Administration Routes. Clays and Clay Minerals, 2016, 64, 115-130.	1.3	74
59	Heterostructured Nanohybrid of Zinc Oxide-Montmorillonite Clay. Journal of Physical Chemistry B, 2006, 110, 1599-1604.	2.6	73
60	Intracrystalline structure of DNA molecules stabilized in the layered double hydroxide. Journal of Physics and Chemistry of Solids, 2006, 67, 1028-1031.	4.0	73
61	Safety Aspect of Inorganic Layered Nanoparticles: Size-Dependency <i>In Vitro</i> and <i>In Vivo</i> . Journal of Nanoscience and Nanotechnology, 2008, 8, 5297-5301.	0.9	73
62	Determination of ionic valency pairs via lattice constants in ordered perovskites (ALa)(Mn2+Mo5+)O6 (A = Ba, Sr, Ca) with applications to (ALa)(Fe3+Mo4+)O6, Ba2(Bi3+Bi5+)O6 and Ba2(Bi3+Sb5+)O6. Journal of Solid State Chemistry, 1977, 20, 233-244.	2.9	71
63	Bio-Resorbable Nanoceramics for Gene and Drug Delivery. MRS Bulletin, 2004, 29, 33-37.	3.5	71
64	Toxicity evaluation of inorganic nanoparticles: considerations and challenges. Molecular and Cellular Toxicology, 2013, 9, 205-210.	1.7	70
65	Toward an Effective Control of the H ₂ to CO Ratio of Syngas through CO ₂ Electroreduction over Immobilized Gold Nanoparticles on Layered Titanate Nanosheets. ACS Catalysis, 2018, 8, 4364-4374.	11.2	69
66	Unilamellar Nanosheet of Layered Manganese Cobalt Nickel Oxide and Its Heterolayered Film with Polycations. ACS Nano, 2010, 4, 4437-4444.	14.6	68
67	LDH Nanocontainers as Bio-Reservoirs and Drug Delivery Carriers. Recent Patents on Nanotechnology, 2012, 6, 200-217.	1.3	68
68	DNA Core@Inorganic Shell. Journal of the American Chemical Society, 2010, 132, 16735-16736.	13.7	67
69	A new single molecular precursor route to fluorine-doped nanocrystalline tin oxide anodes for lithium batteries. Solid State Sciences, 2001, 3, 211-214.	0.7	66
70	Intercalative route to heterostructured nanohybridâ~†. Journal of Physics and Chemistry of Solids, 2004, 65, 373-383.	4.0	64
71	Montmorillonite intercalated with glutathione for antioxidant delivery: Synthesis, characterization, and bioavailability evaluation. International Journal of Pharmaceutics, 2012, 425, 29-34.	5.2	64
72	Cellular uptake and cytotoxicity of octahedral rhenium cluster complexes. Journal of Inorganic Biochemistry, 2008, 102, 1991-1996.	3.5	62

#	Article	IF	CITATIONS
73	New CoOâ^'SiO2-Sol Pillared Clays as Catalysts for NOxConversion. Chemistry of Materials, 2002, 14, 3823-3828.	6.7	61
74	Inorganic Nanovehicle Targets Tumor in an Orthotopic Breast Cancer Model. Scientific Reports, 2014, 4, 4430.	3.3	61
75	Single-Step Synthesis, Characterization, and Application of Nanostructured K <i>_x</i> Mn ₁₋ <i>_y</i> Co <i>_y</i> O ₂₋ _{î´5010-5017.}	sub> 6.7	60
76	New Superconducting Intercalation Compounds: (HgX2)0.5Bi2Sr2CaCu2Oy (X = Br and I). Journal of the American Chemical Society, 1994, 116, 11564-11565.	13.7	59
77	Intra- and inter-layer structures of layered hydroxy double salts, Ni1â^xZn2x(OH)2(CH3CO2)2x•nH2O. Materials Letters, 1998, 34, 356-363.	2.6	59
78	DNA–magnetite nanocomposite materials. Materials Letters, 2000, 42, 183-188.	2.6	59
79	An Inorganic Nanohybrid with High Specific Surface Area:Â TiO2-Pillared MoS2. Chemistry of Materials, 2005, 17, 3492-3498.	6.7	59
80	Low-Temperature Synthesis of LixMn0.67Ni0.33O2 (0.2 <x 0.33)="" <="" a="" hexagonal="" layered<br="" nanowires="" with="">Structure. Advanced Materials, 2005, 17, 2834-2837.</x>	21.0	57
81	CuK-edge x-ray-absorption spectroscopic study on the octahedrally coordinated trivalent copper in the perovskite-related compoundsLa2Li0.5Cu0.5O4andLaCuO3. Physical Review B, 1994, 50, 16631-16639.	3.2	56
82	Nonâ€Hydrothermal Synthesis of 1D Nanostructured Manganeseâ€Based Oxides: Effect of Cation Substitution on the Electrochemical Performance of Nanowires. Advanced Functional Materials, 2007, 17, 2949-2956.	14.9	56
83	PSEUDO-GAP FEATURES OF INTRINSIC TUNNELING IN (HgBr2)-Bi2212 SINGLE CRYSTALS. International Journal of Modern Physics B, 1999, 13, 3758-3763.	2.0	55
84	Electrochromic device of PEDOT–PANI hybrid system for fast response and high optical contrast. Solar Energy Materials and Solar Cells, 2009, 93, 2040-2044.	6.2	55
85	Effects of Chromium Substitution on the Chemical Bonding Nature and Electrochemical Performance of Layered Lithium Manganese Oxide. Journal of Physical Chemistry B, 2000, 104, 7612-7618.	2.6	54
86	Multilayered SiO2/TiO2 Nanosol Particles in Two-Dimensional Aluminosilicate Catalystâ^'Support. Journal of Physical Chemistry B, 1998, 102, 5991-5995.	2.6	53
87	Inoganic–organic-hybrids as precursors to functional materials. Solid State Sciences, 2001, 3, 581-592.	0.7	53
88	Local Atomic Arrangement and Electronic Structure of Nanocrystalline Transition Metal Oxides Determined by X-ray Absorption Spectroscopy. Journal of Physical Chemistry B, 2003, 107, 5791-5796.	2.6	53
89	Microporous SiO2–TiO2 nanosols pillared montmorillonite for photocatalytic decomposition of methyl orange. Journal of Photochemistry and Photobiology A: Chemistry, 2006, 179, 75-80.	3.9	53
90	Chemical Bonding Character and Physicochemical Properties of Mesoporous Zinc Oxide-Layered Titanate Nanocomposites. Journal of Physical Chemistry C, 2007, 111, 1658-1664.	3.1	53

#	Article	IF	CITATIONS
91	Crystal structure and spectroscopic properties of LixNi1 â^' yTiyO2 and their electrochemical behavior. Solid State Ionics, 1996, 86-88, 171-175.	2.7	52
92	New Dionâ^'Jacobson-Type Layered Perovskite Oxyfluorides, ASrNb2O6F (A = Li, Na, and Rb). Chemistry of Materials, 2001, 13, 906-912.	6.7	52
93	Integrated bio-inorganic hybrid systems for nano-forensics. Chemical Society Reviews, 2011, 40, 583-595.	38.1	52
94	Influence of anionic surface modifiers on the thermal stability and mechanical properties of layered double hydroxide/polypropylene nanocomposites. Journal of Materials Chemistry A, 2015, 3, 22730-22738.	10.3	52
95	Synthesis of mesoporous carbons with controlled morphology and pore diameters from SBA-15 prepared through the microwave-assisted process and their CO2 adsorption capacity. Microporous and Mesoporous Materials, 2016, 233, 44-52.	4.4	52
96	Layered Double Hydroxide and Polypeptide Thermogel Nanocomposite System for Chondrogenic Differentiation of Stem Cells. ACS Applied Materials & amp; Interfaces, 2017, 9, 42668-42675.	8.0	52
97	Bio-Nanohybrids Based on Layered Double Hydroxide. Current Nanoscience, 2006, 2, 275-281.	1.2	52
98	Local Crystal Structure around Manganese in New Potassium-Based Nanocrystalline Manganese Oxyiodide. Journal of Physical Chemistry B, 2002, 106, 4053-4060.	2.6	51
99	Effect of physico-chemical parameters on the toxicity of inorganic nanoparticles. Journal of Materials Chemistry, 2011, 21, 5547.	6.7	51
100	Inorganic–inorganic nanohybrids for drug delivery, imaging and photo-therapy: recent developments and future scope. Chemical Science, 2021, 12, 5044-5063.	7.4	51
101	Intercalation of alkylammonium cations into expandable fluorine mica and its application for the evaluation of heterogeneous charge distribution. Journal of Materials Chemistry, 2001, 11, 1305-1312.	6.7	50
102	Anticancer Drug-Inorganic Nanohybrid and Its Cellular Interaction. Journal of Nanoscience and Nanotechnology, 2007, 7, 3700-3705.	0.9	50
103	Hydroxide coprecipitation route to the piezoelectric oxide Pb(Zr,Ti)O3(PZT). Journal of Materials Chemistry, 1995, 5, 65.	6.7	49
104	Synthesis of New Visible Light Active Photocatalysts of Ba(In1/3Pb1/3M1/3â€~ÂÂÂ)O3(Mâ€~ = Nb, Ta): A Band Ga Engineering Strategy Based on Electronegativity of a Metal Component. Journal of Physical Chemistry B, 2005, 109, 15001-15007.	p 2.6	49
105	Intracellular trafficking pathway of layered double hydroxide nanoparticles in human cells: Size-dependent cellular delivery. Applied Clay Science, 2012, 65-66, 24-30.	5.2	49
106	New organo-montmorillonite complexes with hydrophobic and hydrophilic functions. Materials Letters, 1997, 33, 143-147.	2.6	46
107	One step route to the fabrication of arrays of TiO ₂ nanobowls via a complementary block copolymer templating and sol–gel process. Soft Matter, 2008, 4, 515-521.	2.7	46
108	Anionic clay as the drug delivery vehicle: tumor targeting function of layered double hydroxide-methotrexate nanohybrid in C33A orthotopic cervical cancer model. International Journal of Nanomedicine, 2016, 11, 337.	6.7	46

#	Article	IF	CITATIONS
109	Ultra-fine (PMN) powder synthesized from metal-citrate gel by thermal shock method. Materials Research Bulletin, 1990, 25, 283-291.	5.2	45
110	2D Nanostructured Metal Hydroxides with Gene Delivery and Theranostic Functions; A Comprehensive Review. Chemical Record, 2018, 18, 1033-1053.	5.8	45
111	Intracellular Drug Delivery of Layered Double Hydroxide Nanoparticles. Journal of Nanoscience and Nanotechnology, 2011, 11, 1632-1635.	0.9	44
112	Citrate route to the piezoelectric Pb(Zr,Ti)O3 oxide. Journal of Materials Chemistry, 1997, 7, 1815-1820.	6.7	43
113	Biokinetics of zinc oxide nanoparticles: toxicokinetics, biological fates, and protein interaction. International Journal of Nanomedicine, 2014, 9 Suppl 2, 261.	6.7	43
114	2-Dimensional Nanomaterials with Imaging and Diagnostic Functions for Nanomedicine; A Review. Bulletin of the Chemical Society of Japan, 2020, 93, 1-12.	3.2	43
115	Polarization-Dependent X-ray Absorption Spectroscopic Study of [Cu(cyclam)]2+-Intercalated Saponite. Journal of Physical Chemistry B, 2002, 106, 11120-11126.	2.6	42
116	Intercalation of magnesium–urea complex into swelling clay. Journal of Physics and Chemistry of Solids, 2004, 65, 409-412.	4.0	42
117	Effect of Different Forms of Anionic Nanoclays on Cytotoxicity. Journal of Nanoscience and Nanotechnology, 2011, 11, 1803-1806.	0.9	42
118	A novel quantum dot pillared layered transition metal sulfide: CdS–MoS2 semiconductor–metal nanohybrid. Journal of Materials Chemistry, 2002, 12, 614-618.	6.7	41
119	A Latticeâ€Engineering Route to Heterostructured Functional Nanohybrids. Chemistry - an Asian Journal, 2011, 6, 324-338.	3.3	41
120	Intercalation route to nano-hybrids: inorganic/organic-high Tc cuprate hybrid materials. Journal of Materials Chemistry, 1999, 9, 129-135.	6.7	40
121	Enhanced lithium storage capacity and cyclic performance of nanostructured TiO2–MoO3 hybrid electrode. Chemical Communications, 2009, , 7536.	4.1	40
122	Biocompatible ceramic nanocarrier for drug delivery with high efficiency. Journal of the Ceramic Society of Japan, 2009, 117, 543-549.	1.1	40
123	Pre-swelled nanostructured electrode for lithium ion battery: TiO2-pillared layered MnO2. Journal of Materials Chemistry, 2010, 20, 2033.	6.7	40
124	Monolayer Graphitic Carbon Nitride as Metal-Free Catalyst with Enhanced Performance in Photo- and Electro-Catalysis. Nano-Micro Letters, 2022, 14, 55.	27.0	40
125	Phase transition behavior in the perovskite-type layer compound (n-C12H25NH3)2CuCl4. Journal of Physics and Chemistry of Solids, 1993, 54, 1567-1577.	4.0	39
126	Unique phase transformation behavior and visible light photocatalytic activity of titanium oxide hybridized with copper oxide. Journal of Materials Chemistry, 2010, 20, 3238.	6.7	39

#	Article	IF	CITATIONS
127	Hierarchically Ordered Porous CoOOH Thinâ€Film Electrodes for Highâ€Performance Supercapacitors. ChemElectroChem, 2015, 2, 497-502.	3.4	39
128	Stabilization of the Mixed Valence Cu(III)/Cu(IV) in the Perovskite Lattice of La1-xSrxCuO3 under High Oxygen Pressure. Journal of Solid State Chemistry, 1995, 114, 88-94.	2.9	38
129	Effect of Chromium Substitution on the Lattice Vibration of Spinel Lithium Manganate: A New Interpretation of the Raman Spectrum of LiMn2O4. Journal of Physical Chemistry B, 2004, 108, 12713-12717.	2.6	38
130	Inorganic-polymer nanohybrid carrier for delivery of a poorly-soluble drug, ursodeoxycholic acid. International Journal of Pharmaceutics, 2010, 402, 117-122.	5.2	38
131	Drug-inorganic-polymer nanohybrid for transdermal delivery. International Journal of Pharmaceutics, 2013, 444, 120-127.	5.2	38
132	Morphological control of mesoporous CN based hybrid materials and their excellent CO ₂ adsorption capacity. RSC Advances, 2015, 5, 40183-40192.	3.6	38
133	Application of X-ray Absorption Spectroscopy in Determining the Crystal Structure of Low-Dimensional Compounds. Iron Oxychloride and its Alkoxy Substituents. Inorganic Chemistry, 1995, 34, 6524-6531.	4.0	37
134	A combinative flux evaporation–slow cooling route to potassium titanate fibres. Materials Letters, 1998, 34, 111-118.	2.6	37
135	Luminescence of Sr2CeO4. Journal of Luminescence, 2000, 87-89, 1062-1064.	3.1	37
136	LaPdO3: The First PdIIIOxide with the Perovskite Structure. Journal of the American Chemical Society, 2001, 123, 10413-10414.	13.7	37
137	Relationship between Chemical Bonding Character and Electrochemical Performance in Nickel-Substituted Lithium Manganese Oxides. Journal of Physical Chemistry B, 2001, 105, 4860-4866.	2.6	37
138	A new polypyrrole/maghemite hybrid as a lithium insertion electrode. Electrochemistry Communications, 2002, 4, 197-200.	4.7	37
139	Layered titanate–zinc oxide nanohybrids with mesoporosity. Chemical Communications, 2006, , 220-222.	4.1	37
140	P-coumaric acid–zinc basic salt nanohybrid for controlled release and sustained antioxidant activity. Journal of Physics and Chemistry of Solids, 2010, 71, 647-649.	4.0	37
141	Citrate route to ultra-fine barium polytitanates with microwave dielectric properties. Journal of Materials Chemistry, 1995, 5, 57.	6.7	36
142	Crystal structure, magnetism and phase transformation in perovskites A2CrNbO6(A = Ca, Sr, Ba). Journal of the Chemical Society, Faraday Transactions, 1996, 92, 1051.	1.7	36
143	Layered Double Hydroxide as Gene Reservoir. Molecular Crystals and Liquid Crystals, 2000, 341, 425-429.	0.3	36
144	New Solution Route to Electrochromic Poly(acrylic acid)/WO3Hybrid Film. Chemistry of Materials, 2000, 12, 2950-2956.	6.7	36

#	Article	IF	CITATIONS
145	Cellular Toxicity of Inorganic Hydroxide Nanoparticles. Journal of Nanoscience and Nanotechnology, 2007, 7, 4017-4020.	0.9	36
146	Superior role of MXene nanosheet as hybridization matrix over graphene in enhancing interfacial electronic coupling and functionalities of metal oxide. Nano Energy, 2018, 53, 841-848.	16.0	36
147	Acidic and Hydrophobic Microporous Clays Pillared with Mixed Metal Oxide Nano-Sols. Journal of Solid State Chemistry, 1999, 144, 45-52.	2.9	35
148	Photophysical Properties of Hemicyanine Dyes Intercalated in Naâ^'Fluorine Mica. Journal of Physical Chemistry A, 2000, 104, 1388-1392.	2.5	35
149	Micro-Raman Spectroscopic Study on Layered Lithium Manganese Oxide and Its Delithiated/Relithiated Derivatives. Electrochemical and Solid-State Letters, 2001, 4, A213.	2.2	34
150	Soft Chemical Dehydration Route to Carbon Coating of Metal Oxides:  Its Application for Spinel Lithium Manganate. Journal of Physical Chemistry C, 2007, 111, 11347-11352.	3.1	34
151	Encapsulation of Flavor Molecules, 4-Hydroxy-3-Methoxy Benzoic Acid, into Layered Inorganic Nanoparticles for Controlled Release of Flavor. Journal of Nanoscience and Nanotechnology, 2008, 8, 5018-5021.	0.9	34
152	Enhanced thermal stability and mechanical property of EVA nanocomposites upon addition of organo-intercalated LDH nanoparticles. Polymer, 2019, 177, 274-281.	3.8	34
153	Competition of Covalency between CrIII-O and TaV-O Bonds in the Perovskites Ca2CrTaO6 and Sr2CrTaO6. Journal of Solid State Chemistry, 1994, 111, 370-379.	2.9	33
154	Citrate Route to Snâ€Doped BaTi4O9 with Microwave Dielectric Properties. Journal of the American Ceramic Society, 1998, 81, 3197-3204.	3.8	33
155	Intercalative route to heterostructured nanohybrids. Current Applied Physics, 2002, 2, 489-495.	2.4	33
156	AripiprazoleMontmorillonite: A New Organic–Inorganic Nanohybrid Material for Biomedical Applications. Chemistry - A European Journal, 2013, 19, 4869-4875.	3.3	33
157	TiO ₂ -pillared clays with well-ordered porous structure and excellent photocatalytic activity. RSC Advances, 2015, 5, 8210-8215.	3.6	33
158	Soft XAFS study on the 4d electronic structure of ruthenium in complex perovskite oxide. Solid State Sciences, 2000, 2, 61-70.	0.7	31
159	Variation of the Chemical Bonding Nature of LiMn2-xNixO4Spinel Oxides upon Delithiation and Lithiation Reactions. Journal of Physical Chemistry B, 2001, 105, 335-342.	2.6	31
160	Structural Distortion and Chemical Bonding in TlFeO3: Comparison with AFeO3 (A=Rare Earth). Journal of Solid State Chemistry, 2001, 161, 197-204.	2.9	31
161	Soft-solution route to ZnO nanowall array with low threshold power density. Applied Physics Letters, 2010, 97, 043109.	3.3	31
162	Intracrystalline structure and release pattern of ferulic acid intercalated into layered double hydroxide through various synthesis routes. Applied Clay Science, 2015, 112-113, 32-39.	5.2	31

#	Article	IF	CITATIONS
163	Ultrafast humidity-responsive structural colors from disordered nanoporous titania microspheres. Journal of Materials Chemistry A, 2019, 7, 10561-10571.	10.3	31
164	High pressure synthesis and crystal structure of a new Ni(III) perovskite: TlNiO3. Journal of Materials Chemistry, 2001, 11, 487-492.	6.7	30
165	Temperature-dependent structural evolution and electrochromic properties of peroxopolytungstic acid. Journal of Materials Chemistry, 2001, 11, 1506-1513.	6.7	30
166	Poly(3,4-ethylenedioxythiophene)V2O5 hybrids for lithium batteries. Electrochemistry Communications, 2002, 4, 384-387.	4.7	30
167	Nanocrystalline Sodalite from Al2O3 Pillared Clay by Solidâ^'Solid Transformation. Chemistry of Materials, 2003, 15, 4841-4845.	6.7	30
168	Intracrystalline Structure and Physicochemical Properties of Mixed SiO2â^'TiO2Sol-Pillared Aluminosilicate. Journal of Physical Chemistry B, 2006, 110, 1592-1598.	2.6	30
169	Highly Condensed Boron Cage Cluster Anions in 2D Carrier and Its Enhanced Antitumor Efficiency for Boron Neutron Capture Therapy. Advanced Functional Materials, 2018, 28, 1704470.	14.9	30
170	X-Ray absorption spectroscopic study on LaPdO3. Journal of Materials Chemistry, 2002, 12, 995-1000.	6.7	29
171	Exfoliation–restacking route to Au nanoparticle-clay nanohybrids. Journal of Physics and Chemistry of Solids, 2006, 67, 1020-1023.	4.0	29
172	Drugâ€Ceramic 2â€Dimensional Nanoassemblies for Drug Delivery System in Physiological Condition. Journal of the American Ceramic Society, 2012, 95, 2758-2765.	3.8	29
173	Recent trends in nano photo-chemo therapy approaches and future scopes. Coordination Chemistry Reviews, 2020, 411, 213252.	18.8	29
174	Intracrystalline and Electronic Structures of Copper(II) Complexes Stabilized in Two-Dimensional Aluminosilicate. Inorganic Chemistry, 1997, 36, 189-195.	4.0	28
175	Structural and electrochemical properties of the spinel Li(Mn2â^'xLix/4Co3x/4)O4. Solid State Ionics, 2001, 139, 75-81.	2.7	28
176	Origin of Improved Electrochemical Activity of β-MnO ₂ Nanorods: Effect of the Mn Valence in the Precursor on the Crystal Structure and Electrode Activity of Manganates. Journal of Physical Chemistry C, 2009, 113, 21274-21282.	3.1	28
177	Avatar DNA Nanohybrid System in Chip-on-a-Phone. Scientific Reports, 2014, 4, 4879.	3.3	28
178	A Study of the Nonstoichiometry and Physical Properties of the Perovskite Nd1-xCaxFeO3-y System. Journal of Solid State Chemistry, 1995, 114, 265-270.	2.9	27
179	X-Ray absorption spectroscopic and electrochemical analyses of Pt–Cu–Fe ternary alloy electrocatalysts supported on carbon. Journal of the Chemical Society, Faraday Transactions, 1998, 94, 2835-2841.	1.7	27
180	Synthesis of porous and nonporous ZnO nanobelt, multipod, and hierarchical nanostructure from Zn-HDS. Journal of Solid State Chemistry, 2010, 183, 1835-1840.	2.9	27

#	Article	IF	CITATIONS
181	Theranostic Bioabsorbable Bone Fixation Plate with Drug‣ayered Double Hydroxide Nanohybrids. Advanced Healthcare Materials, 2016, 5, 2765-2775.	7.6	27
182	In Vivo Anticancer Activity of Methotrexate-loaded Layered Double Hydroxide Nanoparticles. Current Pharmaceutical Design, 2013, 19, 7196-7202.	1.9	27
183	Layered double hydroxides as potential solid base for beneficial remediation of endosulfan-contaminated soils. Journal of Physics and Chemistry of Solids, 2004, 65, 513-516.	4.0	26
184	Influences of A- and B-site cations on the physicochemical properties of perovskite-structured A(In1/3Nb1/3B1/3)O3 (A=Sr, Ba; B=Sn, Pb) photocatalysts. Journal of Photochemistry and Photobiology A: Chemistry, 2006, 183, 176-181.	3.9	26
185	Vacuum seeding and secondary growth route to sodalite membrane. Thin Solid Films, 2006, 495, 92-96.	1.8	26
186	Optical iris application of electrochromic thin films. Electrochemistry Communications, 2008, 10, 1785-1787.	4.7	26
187	Intercalative Ionâ€Exchange Route to Amino Acid Layered Double Hydroxide Nanohybrids and Their Sorption Properties. European Journal of Inorganic Chemistry, 2015, 2015, 925-930.	2.0	26
188	X-ray diffraction and X-ray absorption spectroscopic analyses for intercalative nanohybrids with low crystallinity. Arabian Journal of Chemistry, 2016, 9, 190-205.	4.9	26
189	X-ray Absorption Spectroscopic Evidence on the Partial Formation of Copper(III) in the Superconducting La2CuO4.08. Journal of the American Chemical Society, 1995, 117, 7556-7557.	13.7	25
190	One-pot synthetic route to polymer–silica assembled capsule encased with nonionic drug molecule. Chemical Communications, 2007, , 2799-2801.	4.1	25
191	Superionic and Superconducting Nanohybrids with Heterostructure, AgxIwBi2Sr2Can-1CunOy(0.76 ≤â‰)¤T	j ET <u>Q</u> g1 1 2.6	0.784314 rg 24
192	Modification of the interlayer pore structure of silica iron oxide sol pillared clay using organic templates. Journal of Materials Chemistry, 1998, 8, 1459-1463.	6.7	24
193	Highly Ordered Nanoporous Carbon Films with Tunable Pore Diameters and their Excellent Sensing Properties. Chemistry - A European Journal, 2015, 21, 697-703.	3.3	24
194	A novel geopolymer route to porous carbon: high CO ₂ adsorption capacity. Chemical Communications, 2019, 55, 3266-3269.	4.1	24
195	Electrochemical property of surface modified polypyrrole film with heteropoly anions. Synthetic Metals, 1995, 69, 481-482.	3.9	23
196	Charge Transfer–TcRelation in the Superconducting Intercalates IBi2Sr2CaCu2Oy. Journal of Solid State Chemistry, 1998, 138, 66-73.	2.9	23
197	A new approach for the synthesis of layered niobium sulfide and restacking route of NbS2 nanosheet. Journal of Solid State Chemistry, 2008, 181, 319-324.	2.9	23
198	Gadolinium (III) Diethylenetriamine Pentaacetic Acid/Layered Double Hydroxide Nanohybrid as Novel T ₁ -Magnetic Resonant Nanoparticles. Journal of Nanoscience and Nanotechnology, 2008, 8, 5181-5184.	0.9	23

#	Article	IF	CITATIONS
199	A Dualâ€Polymer Electrochromic Device with High Coloration Efficiency and Fast Response Time: Poly(3,4â€(1,4â€butyleneâ€(2â€ene)dioxy)thiophene)–Polyaniline ECD. Chemistry - an Asian Journal, 2011, 6, 2123-2129.	3.3	23
200	A nanohybrid system for taste masking of sildenafil. International Journal of Nanomedicine, 2012, 7, 1635.	6.7	23
201	Mesoporous BN and BCN nanocages with high surface area and spherical morphology. Physical Chemistry Chemical Physics, 2014, 16, 23554-23557.	2.8	23
202	Doxorubicin Encapsulated in TPGSâ€Modified 2Dâ€Nanodisks Overcomes Multidrug Resistance. Chemistry - A European Journal, 2020, 26, 2470-2477.	3.3	23
203	Recent progress in layered double hydroxides as a cancer theranostic nanoplatform. Wiley Interdisciplinary Reviews: Nanomedicine and Nanobiotechnology, 2021, 13, e1679.	6.1	23
204	Study of the electronic structural variation of transition metal oxides by X-ray absorption spectroscopy. Solid State Ionics, 1998, 108, 159-163.	2.7	22
205	Trigonal Planar (D3h) AuI3Complex Stabilized in a Solid Lattice. Journal of Physical Chemistry B, 2000, 104, 7273-7277.	2.6	22
206	CoK-edge XAS study on a new cobalt-doped-SiO2pillared clay. Journal of Synchrotron Radiation, 2001, 8, 599-601.	2.4	22
207	The orientation of anionic β-cyclodextrin in the interlayer space of Zn/Al layered double hydroxide. Journal of Physics and Chemistry of Solids, 2004, 65, 509-512.	4.0	22
208	Nanostructured TiO2 films for dye-sensitized solar cells. Journal of Physics and Chemistry of Solids, 2006, 67, 1308-1311.	4.0	22
209	Fabrication of YBa2Cu3O7a^^î´superconducting nanofibres by electrospinning. Superconductor Science and Technology, 2006, 19, 1264-1268.	3.5	22
210	A vanadate (V) oxide with perovskite structure: La2LiVO6, comparison with homologous La2LiMO6 phases (M = Fe, Nb, Mo, Ru, Ta, Re, Os, Ir). Materials Research Bulletin, 1987, 22, 735-740.	5.2	21
211	Unusual High Oxidation State of Iodine Intercalated in the Bi2Sr2CaCu2Ox Superconductor. Journal of Solid State Chemistry, 1993, 102, 284-287.	2.9	21
212	Physico-Chemical Characterization of Na3Zr2Si2PO12Fine Powders Prepared by Sol-Gel Method Using Citrates. Japanese Journal of Applied Physics, 1993, 32, 1154-1159.	1.5	21
213	Molecular layer-by-layer engineering of superconducting and superionic materials in the (AgI)Bi2Sr2CaCu2Oy system. The Journal of Physical Chemistry, 1995, 99, 7845-7848.	2.9	21
214	Oxalate coprecipitation route to the piezoelectric Pb(Zr,Ti)O3 oxide. Journal of Materials Chemistry, 1997, 7, 1807-1813.	6.7	21
215	Influence of nickel content on the chemical bonding character of LiMn2â^'xNixO4 spinel oxides. Journal of Power Sources, 2006, 159, 1346-1352.	7.8	21
216	Characterization and Stability Analysis of Zinc Oxide Nanoencapsulated Conjugated Linoleic Acid. Journal of Food Science, 2010, 75, N63-8.	3.1	21

#	Article	IF	CITATIONS
217	Enabling Nanohybrid Drug Discovery through the Soft Chemistry Telescope. Industrial & Engineering Chemistry Research, 2016, 55, 11211-11224.	3.7	21
218	Recent Developments on Semiconducting Polymer Nanoparticles as Smart Photo-Therapeutic Agents for Cancer Treatments—A Review. Polymers, 2021, 13, 981.	4.5	21
219	Niclosamide–Clay Intercalate Coated with Nonionic Polymer for Enhanced Bioavailability toward COVID-19 Treatment. Polymers, 2021, 13, 1044.	4.5	21
220	A new thermally stable SiO2–Cr2O3 sol pillared montmorillonite with high surface area. Applied Catalysis A: General, 1998, 174, 83-90.	4.3	20
221	A Novel Hybrid of Bi-Based High-TcSuperconductor and Molecular Complex. Inorganic Chemistry, 2003, 42, 8134-8136.	4.0	20
222	Formation Efficiency of One-Dimensional Nanostructured Titanium Oxide Affected by the Structure and Composition of Titanate Precursor: A Mechanism Study. Journal of Physical Chemistry C, 2008, 112, 15966-15972.	3.1	20
223	Enhancing the UV A1 screening ability of caffeic acid by encapsulation in layered basic zinc hydroxide matrix. Journal of Physics and Chemistry of Solids, 2012, 73, 1510-1513.	4.0	20
224	Clay-organic intumescent hybrid system for the synergetic flammability of polymer nanocomposites. Journal of Thermal Analysis and Calorimetry, 2018, 132, 2009-2014.	3.6	20
225	Implantable multireservoir device with stimulus-responsive membrane for on-demand and pulsatile delivery of growth hormone. Proceedings of the National Academy of Sciences of the United States of America, 2019, 116, 201906931.	7.1	20
226	Effect of organo-smectite clays on the mechanical properties and thermal stability of EVA nanocomposites. Applied Clay Science, 2020, 196, 105750.	5.2	20
227	Layered Metal Hydroxides Containing Calcium and Their Structural Analysis. Bulletin of the Korean Chemical Society, 2012, 33, 1845-1850.	1.9	20
228	Evolution of Superconducting Transition Temperature (Tc) upon Intercalation of HgBr2into the Bi2Sr1.5-xLaxCa1.5Cu2Oy. The Journal of Physical Chemistry, 1996, 100, 3783-3787.	2.9	19
229	B-site cation arrangement and crystal structure of layered perovskite compounds CsLn2Ti2NbO10 (Ln =) Tj ETQq	1 <u>1 0</u> .784 6.7	314 rgBT /○ 19
230	Neutron Diffraction and X-ray Absorption Spectroscopic Analyses for Lithiated Aurivillius-Type Layered Perovskite Oxide, Li2Bi4Ti3O12. Journal of Physical Chemistry B, 2001, 105, 7908-7912.	2.6	19
231	Variation of chemical bonding nature of layered LiMnO2 upon delithiation/relithiation and Cr substitution. Solid State Ionics, 2002, 151, 275-283.	2.7	19
232	Gold Valence in (AuI3)0.25Bi2Sr2CaCu2Oyby XPS and XANES Spectroscopy. Journal of Physical Chemistry B, 2003, 107, 3348-3350.	2.6	19
233	Nanohybrids of edible dyes intercalated in ZnAl layered double hydroxides. Journal of Physics and Chemistry of Solids, 2008, 69, 1547-1551.	4.0	19
234	Generating Color from Polydisperse, Near Micron-Sized TiO ₂ Particles. ACS Applied Materials & Interfaces, 2017, 9, 23941-23948.	8.0	19

#	Article	IF	CITATIONS
235	Atomic and electronic structures of graphene-decorated graphitic carbon nitride (g-C3N4) as a metal-free photocatalyst under visible-light. Applied Catalysis B: Environmental, 2019, 256, 117850.	20.2	19
236	Citrate route to the preparation of nanometer size (Pb, La) (Zr, Ti) O3 oxide. Materials Letters, 1997, 32, 209-215.	2.6	18
237	Soft-solution route to various ZnO nanoplate arrays. CrystEngComm, 2010, 12, 3467.	2.6	18
238	Porous SnO ₂ /layered titanate nanohybrid with enhanced electrochemical performance for reversible lithium storage. Chemical Communications, 2012, 48, 458-460.	4.1	18
239	Citrate sol-gel method for the preparation of $\hat{I}^2 \hat{I}^2 \hat{a} \in 2^{\prime}$ -alumina. Materials Letters, 1993, 16, 226-230.	2.6	17
240	Soft Chemical Routes to Heterostructured High-T _c Superconducting Materials. MRS Bulletin, 2000, 25, 32-39.	3.5	17
241	Coherent mode splitting of microwave-induced fluxons inHgl2â^'intercalatedBi2Sr2CaCu2O8+Î′single crystals. Physical Review B, 2001, 63, .	3.2	17
242	Tailoring the Mesoporous Texture of Graphitic Carbon Nitride. Journal of Nanoscience and Nanotechnology, 2013, 13, 7487-7492.	0.9	17
243	2D Inorganic–Antimalarial Drug–Polymer Hybrid with pHâ€Responsive Solubility. Chemistry - an Asian Journal, 2015, 10, 2264-2271.	3.3	17
244	Bio-Layered Double Hydroxides Nanohybrids for Theranostics Applications. Structure and Bonding, 2015, , 137-175.	1.0	17
245	Highly Stable Nanocontainer of APTES-Anchored Layered Titanate Nanosheet for Reliable Protection/Recovery of Nucleic Acid. Scientific Reports, 2016, 6, 21993.	3.3	17
246	Alendronate-Anionic Clay Nanohybrid for Enhanced Osteogenic Proliferation and Differentiation. Journal of Korean Medical Science, 2019, 34, e37.	2.5	17
247	Low-Dimensional and Extended Metal—Metal Bonded Networks in Transition Metal Compounds: Ba2Nb5O9, Ba2-xYxNb5O9. Journal of Solid State Chemistry, 1994, 108, 253-259.	2.9	16
248	Iridium(III) stabilized in oxygen lattices with the perovskite structure Sr2Mlr III O6(M = Nb, Ta). Journal of Materials Chemistry, 1995, 5, 517.	6.7	16
249	Synthesis and characterization of porous ferrimagnetic membranes. Microporous and Mesoporous Materials, 2003, 63, 177-184.	4.4	16
250	Nanostructured Metal Surfaces Fabricated by a Nonlithographic Template Method. Langmuir, 2004, 20, 287-290.	3.5	16
251	Effects of p- and d-block metal co-substitution on the electronic structure and physicochemical properties of InMO4 (M=Nb and Ta) semiconductors. Chemical Physics Letters, 2007, 434, 251-255.	2.6	16
252	Dynamic transition between Zn-HDS and ZnO; growth and dissolving mechanism of dumbbell-like ZnO bipod crystal. CrystEngComm, 2011, 13, 546-552.	2.6	16

#	Article	IF	CITATIONS
253	Bovine Serum Albumin-Coated Niclosamide-Zein Nanoparticles as Potential Injectable Medicine against COVID-19. Materials, 2021, 14, 3792.	2.9	16
254	2D→3D transformation of layered aluminosilicate upon base treatment. Solid State Ionics, 2002, 151, 343-346.	2.7	15
255	Solid–solid transformation mechanism for nanocrystalline sodalite from pillared clay. Chemical Communications, 2003, , 1922-1923.	4.1	15
256	Zr K-Edge XAS and ²⁹ Si MAS NMR Studies on Hexagonal Mesoporous Zirconium Silicate. Journal of Porous Materials, 2004, 11, 123-129.	2.6	15
257	The isopropylation of naphthalene with propene over H-mordenite: The catalysis at the internal and external acid sites. Journal of Molecular Catalysis A, 2014, 395, 543-552.	4.8	15
258	Stabilization of antioxidant gallate in layered double hydroxide by exfoliation and reassembling reaction. Solid State Sciences, 2018, 80, 65-71.	3.2	15
259	In Situ X-ray Absorption Spectroscopic Study for α-MoO ₃ Electrode upon Discharge/Charge Reaction in Lithium Secondary Batteries. Bulletin of the Korean Chemical Society, 2010, 31, 3675-3678.	1.9	15
260	The emergence of nanoporous materials in lung cancer therapy. Science and Technology of Advanced Materials, 2022, 23, 225-274.	6.1	15
261	N-alkylammonium intercalated 2-d hydrous titanates and their thermotropic phase transition. Synthetic Metals, 1995, 71, 2053-2054.	3.9	14
262	X-ray Absorption Near-Edge Structure (XANES) of Iodine Intercalated C60: Evidence of I2δ+in I2C60. Chemistry of Materials, 1996, 8, 324-326.	6.7	14
263	Raman spectroscopic evidence on molecular mercuric bromide in the two-dimensional lattice of (HgBr2)0.5Bi2Sr2CaCu2Oys. Physical Review B, 1997, 55, 5674-5677.	3.2	14
264	In situXAFS study at the ZrK-edge for SiO2/ZrO2nano-sol. Journal of Synchrotron Radiation, 2001, 8, 782-784.	2.4	14
265	Substitution effect of pentavalent bismuth ions on the electronic structure and physicochemical properties of perovskite-structured Ba(In0.5Ta0.5â°'xBix)O3 semiconductors. Materials Research Bulletin, 2007, 42, 1914-1920.	5.2	14
266	Intercalative hybridization of layered double hydroxide nanocrystals with mesoporous g-C ₃ N ₄ for enhancing visible light-induced H ₂ production efficiency. Dalton Transactions, 2018, 47, 2949-2955.	3.3	14
267	Most facile synthesis of Zn-Al:LDHs nanosheets at room temperature via environmentally friendly process and their high power generation by flexoelectricity. Materials Today Energy, 2018, 10, 254-263.	4.7	14
268	Hydrotalcite–Niclosamide Nanohybrid as Oral Formulation towards SARS-CoV-2 Viral Infections. Pharmaceuticals, 2021, 14, 486.	3.8	14
269	Niclosamide encapsulated in mesoporous silica and geopolymer: A potential oral formulation for COVID-19. Microporous and Mesoporous Materials, 2021, 326, 111394.	4.4	14
270	Structure and Physical Properties of the Barium Niobium Sulfides BaNbS3 and BaNb0.8S3-δ. Journal of Solid State Chemistry, 1995, 115, 427-434.	2.9	13

#	Article	IF	CITATIONS
271	Effect ofHgl2intercalation onBi2Sr2CaCu2Oy: Interlayer coupling effect. Physical Review B, 1996, 53, 12416-12421.	3.2	13
272	Local Atomic Arrangement and Electronic Configuration of Nanocrystalline Zinc Oxide Hybridized with Redoxable 2D Lattice of Manganese Oxide. Journal of Physical Chemistry C, 2007, 111, 16774-16780.	3.1	13
273	Zr K-edge XAS study on ZrO2-pillared aluminosilicate. Journal of Porous Materials, 2007, 14, 369-377.	2.6	13
274	Fe ₃ O ₄ @ Polypyrrole Core–Shell Nanohybrid for Efficient DNA Retrieval. Journal of Nanoscience and Nanotechnology, 2008, 8, 5014-5017.	0.9	13
275	Relationship between Electrode Performance and Chemical Bonding Nature in Mesoporous Metal Oxide-Layered Titanate Nanohybrids. Journal of Physical Chemistry C, 2009, 113, 21941-21948.	3.1	13
276	Pt Nanoparticle-Reduced Graphene Oxide Nanohybrid for Proton Exchange Membrane Fuel Cells. Journal of Nanoscience and Nanotechnology, 2012, 12, 5669-5672.	0.9	13
277	Highly Enhanced Photocatalytic Water-Splitting Activity of Gallium Zinc Oxynitride Derived from Flux-Assisted Zn/Ga Layered Double Hydroxides. Industrial & Engineering Chemistry Research, 2018, 57, 16264-16271.	3.7	13
278	Physicochemical distinction between Cu3+ and O22- in YBa2Cu3O6.5+l̂´lattice upon oxidation reaction of bremide and spectroscopic analyses. Physica C: Superconductivity and Its Applications, 1991, 185-189, 763-764.	1.2	12
279	A new high-Tc superconducting intercalation compound. Synthetic Metals, 1995, 71, 1551-1553.	3.9	12
280	Grafting Mechanism of Electrochromic PAA–WO3Composite Film. Journal of Solid State Chemistry, 1999, 142, 368-373.	2.9	12
281	Heterostructured high-Tcsuperconducting nanohybrid:(Me3S)2HgI4â^'Bi2Sr2CaCu2Oy. Physical Review B, 2002, 66, .	3.2	12
282	Transformation from Microcrystalline LiMn1-xCrxO2 to 1D Nanostructured β-Mn1-xCrxO2:  Promising Electrode Performance of β-MnO2-Type Nanowires. Journal of Physical Chemistry C, 2008, 112, 5160-5164.	3.1	12
283	CeO2-layered aluminosilicate nanohybrids for UV screening. Journal of Physics and Chemistry of Solids, 2012, 73, 1478-1482.	4.0	12
284	Photoluminescent nanographitic/nitrogen-doped graphitic hollow shells as a potential candidate for biological applications. Journal of Materials Chemistry B, 2013, 1, 1229.	5.8	12
285	Titania Nanoparticles Stabilized HPA in SBAâ€15 for the Intermolecular Hydroamination of Activated Olefins. ChemCatChem, 2014, 6, 3347-3354.	3.7	12
286	Preparation of Highly Active Triflic Acid Functionalized SBAâ€15 Catalysts for the Synthesis of Coumarin under Solventâ€Free Conditions. ChemCatChem, 2016, 8, 336-344.	3.7	12
287	Brimonidine–montmorillonite hybrid formulation for topical drug delivery to the eye. Journal of Materials Chemistry B, 2020, 8, 7914-7920.	5.8	12
288	Cellular Toxicity of Inorganic Hydroxide Nanoparticles. Journal of Nanoscience and Nanotechnology, 2007, 7, 4017-4020.	0.9	12

#	Article	IF	CITATIONS
289	Selective DNA Adsorption on Layered Double Hydroxide Nanoparticles. Bulletin of the Korean Chemical Society, 2011, 32, 2217-2221.	1.9	12
290	High-pressure synthesis of cubic perovskite CaLaMgMnO5.5+x. Journal of Solid State Chemistry, 1990, 84, 1-9.	2.9	11
291	A spectroscopic study on the existence of Cu3+ OR O2â^'2 in the superconducting YBa2Cu3â^'xCoxO7±δ phase. Journal of Physics and Chemistry of Solids, 1991, 52, 545-549.	4.0	11
292	Structural evolution of SiO2–ZrO2 nano-sol intercalated clays upon pillaring reactionElectronic supplementary information (ESI) available: BJH pore size distribution and k3-weighted EXAFS spectra of the SiO2–ZrO2 sol-pillared clay at different calcination temperatures. See http://www.rsc.org/suppdata/jm/b2/b208929g/. Journal of Materials Chemistry, 2003, 13, 557-562.	6.7	11
293	Cationic and Anionic Clays for Biological Applications. Interface Science and Technology, 2004, 1, 403-424.	3.3	11
294	Asymmetric High-TcSuperconducting Gas Separation Membrane. Chemistry of Materials, 2007, 19, 3840-3844.	6.7	11
295	Mesoporous Carbons Functionalized with Aromatic, Aliphatic, and Cyclic Amines, and their Superior Catalytic Activity. ChemCatChem, 2014, 6, 2872-2880.	3.7	11
296	Water-floating nanohybrid films of layered titanate–graphene for sanitization of algae without secondary pollution. RSC Advances, 2016, 6, 98528-98535.	3.6	11
297	Inorganic Nanomedicines and their Labeling for Biological Imaging. Current Topics in Medicinal Chemistry, 2013, 13, 488-503.	2.1	11
298	lr, Raman, and X-ray photoelectron spectroscopy investigations of the ordered cubic perovskite La2LiVO6. Journal of Solid State Chemistry, 1988, 76, 97-101.	2.9	10
299	Preparation of new intercalation complexes of n-alkylamines with FeMoO4Cl and electrochemical lithiation of FeMoO4Cl. Materials Research Bulletin, 1988, 23, 73-86.	5.2	10
300	A new perovskite-type oxide (BaLa)(MgMn)O6â^'x(xâ‰0.21) prepared under high oxygen pressure and its physico-chemical characterization. Journal of Physics and Chemistry of Solids, 1990, 51, 391-396.	4.0	10
301	Stabilization of Fe(V) as substituting element in the La2LiVO6 perovskite lattice. Solid State Communications, 1991, 77, 647-649.	1.9	10
302	Local Distortion and Chemical Surroundings of \$f NiO_{6}\$ Octahedra for Ni(III) Oxides with \$f K_{2}NiF_{4}\$-Type Structure. Japanese Journal of Applied Physics, 1995, 34, 6156-6163.	1.5	10
303	X-Ray Absorption Near Edge Structure and X-Ray Diffraction Studies of New Cubic CsVTeO5and CsVTeO6Compounds. Japanese Journal of Applied Physics, 1999, 38, 1506-1509.	1.5	10
304	Heterostructured Bi-Based Cuprate High-Tc Superconductors with Unusually Coordinated Metal Halides. Journal of Solid State Chemistry, 1999, 147, 328-335.	2.9	10
305	The Ni(III) perovskites: synthesis under high oxygen pressures and physico-chemical properties. Solid State Communications, 2000, 117, 113-115.	1.9	10
306	Pseudogap features of intrinsic tunneling in Bi2212 single crystals. Physica C: Superconductivity and Its Applications, 2001, 362, 286-289.	1.2	10

#	Article	IF	CITATIONS
307	Direct Softâ€Chemical Synthesis of Chalcogenâ€Doped Manganese Oxide 1D Nanostructures: Influence of Chalcogen Doping on Electrode Performance. Small, 2008, 4, 507-514.	10.0	10
308	Vectorized Clay Nanoparticles in Therapy and Diagnosis. Clays and Clay Minerals, 2019, 67, 25-43.	1.3	10
309	Chitosan hybrids for cosmeceutical applications in skin, hair and dental care: an update. Emergent Materials, 2021, 4, 1125-1142.	5.7	10
310	Ketoprofen-LDH Nanohybrid for Transdermal Drug Delivery System. Bulletin of the Korean Chemical Society, 2012, 33, 1827-1828.	1.9	10
311	Preparation of 90K superconductor YBa2Cu3O7â^î^ via oxide precursors BaCuO2 and Y2Cu2O5. Materials Research Bulletin, 1989, 24, 867-874.	5.2	9
312	Preparation of single-phase Pb(Mg1/3Nb2/3)O3samples utilizing information from solubility relationships in the Pb–Mg–Nb–citric acid–H2O system. Journal of Materials Chemistry, 1994, 4, 1271-1274.	6.7	9
313	4dElectronic structure analysis of ruthenium in the perovskite oxides by RuK- andL-edge XAS. Journal of Synchrotron Radiation, 2001, 8, 722-724.	2.4	9
314	Electron Paramagnetic Resonance Study of Partially Oriented Clay Platelets Intercalated with Copper(II) 1,4,8,11-Tetraazacyclotetradecane. Journal of Physical Chemistry B, 2005, 109, 3324-3329.	2.6	9
315	Evidence of Two-Dimensional Superconductivity in the Single Crystalline Nanohybrid of Organic-Bismuth Cuprate. Journal of Physical Chemistry B, 2006, 110, 16197-16200.	2.6	9
316	Synthesis of large ring 3,4-alkylenedioxythiophenes (ADOT) derivatives via Mitsunobu reaction. Tetrahedron Letters, 2011, 52, 2823-2825.	1.4	9
317	Facile Synthesis of Crystalline Nanoporous GaN Templated by Nitrogen Enriched Mesoporous Carbon Nitride for Friedel rafts Reaction. ChemistrySelect, 2016, 1, 6062-6068.	1.5	9
318	High Pressure Synthesis of a New Perovskite, (SrLa)(MgMn)O6-x. Japanese Journal of Applied Physics, 1992, 31, 3649-3654.	1.5	8
319	X-ray absorption spectroscopic studies on the iridium(III) complexes. Materials Letters, 1998, 37, 168-175.	2.6	8
320	Synthesis and characterization of porous inorganic membranes exhibiting superconducting properties. Materials Chemistry and Physics, 2004, 84, 348-357.	4.0	8
321	Porous ceramic membranes exhibiting ferri/ferromagnetic properties for separation. Separation and Purification Technology, 2005, 46, 118-124.	7.9	8
322	Effect of Bond Covalency on the Lattice Stability and Fatigue Behavior of Ferroelectric Bismuth Transition-Metal Oxides. Journal of Physical Chemistry C, 2008, 112, 3434-3438.	3.1	8
323	New Antimony Substituted Mg-Al Layered Double Hydroxides. Journal of Nanoscience and Nanotechnology, 2008, 8, 5172-5175.	0.9	8
324	Biodegradable Inorganic Nanovector: Passive versus Active Tumor Targeting in siRNA Transportation. Angewandte Chemie, 2016, 128, 4658-4662.	2.0	8

#	Article	IF	CITATIONS
325	Polylactic Acid/Chitosan Nanoparticles Loading Nifedipine: Characterization Findings and <i>In Vivo</i> Investigation in Animal. Journal of Nanoscience and Nanotechnology, 2018, 18, 2294-2303.	0.9	8
326	A geopolymer route to micro- and meso-porous carbon. RSC Advances, 2020, 10, 6814-6821.	3.6	8
327	Hematocompatibility and Interaction of Layered Double Hydroxide Nanomaterials with Plasma Proteins. Science of Advanced Materials, 2014, 6, 1582-1589.	0.7	8
328	X-ray diffraction, differential scanning calorimetry, and spectroscopic studies of phase transitions in FeOCl-n-alkylamine intercalation complexes. Journal of Solid State Chemistry, 1988, 77, 60-66.	2.9	7
329	Influence of competing bonds along the c-axis on the local distortion of the (CoO6) octahedron in K2NiF4-type oxides A′0.50La1.50Mg0.50Co0.50O4 (A′ = Ca, Sr and Ba). Solid State Communications, 1991 457-463.	, 8.0,	7
330	High spin FeIV stabilized in the La LiVo perovskite lattice under high pressure. Solid State Communications, 1991, 80, 683-686.	1.9	7
331	In situtemperature-dependent x-ray-absorption spectroscopic studies for the mercury-based superconductors. Physical Review B, 1998, 57, 1259-1265.	3.2	7
332	HRTEM and Micro-Raman Studies on Superconducting☒Superionic Conducting Nanohybrid, Ag1.17I1.54Bi2Sr2CaCu2Oy. Journal of Physical Chemistry B, 2000, 104, 9086-9090.	2.6	7
333	Solid–solid transformation route to nanocrystalline sodalite from Al-PILC at room temperature. Journal of Physics and Chemistry of Solids, 2004, 65, 421-424.	4.0	7
334	High-Tc superconducting thin film from bismuth cuprate nano-colloids. Thin Solid Films, 2006, 495, 78-81.	1.8	7
335	Emerging Strategies in Infohybrid Systems. European Journal of Inorganic Chemistry, 2012, 2012, 5145-5143.	2.0	7
336	Heterostructured Layered Aluminosilicate-Itraconazole Nanohybrid for Drug Delivery System. Journal of Nanoscience and Nanotechnology, 2013, 13, 7331-7336.	0.9	7
337	Injectable niclosamide nanohybrid as an anti-SARS-CoV-2 strategy. Colloids and Surfaces B: Biointerfaces, 2021, 208, 112063.	5.0	7
338	Infrared absorption investigations of the ALa3MgCoO8 (A = Ca, Sr, Ba) oxides. Journal of Solid State Chemistry, 1989, 80, 40-44.	2.9	6
339	Citrate sol-gel route to high Tc superconducting Yî—,Baî—,Cuî—,O fiber. Physica C: Superconductivity and Its Applications, 1991, 185-189, 511-512.	1.2	6
340	A new cointercalated superconducting bismuth cuprate, (Hgl2)0.5l0.5Bi1.85Pb0.35Sr1.9Ca2.1Cu3.1O10 + δ. Journal of Materials Chemistry, 2000, 10, 1679-1684.	6.7	6
341	Polarized XANES study of the importance of inter-block vis-\$agrave\$-vis intra-block coupling in evolution of Tc in halide-molecule-intercalated Bi2Sr2CaCu2O8\$minus\$\$delta\$ single crystals. Journal of Physics Condensed Matter, 2002, 14, 6675-6688.	1.8	6
342	Effect of reaction media on electrochemical performance of nanocrystalline manganese oxyiodides prepared by Chimie Douce route. Journal of Power Sources, 2004, 125, 119-123.	7.8	6

#	Article	IF	CITATIONS
343	Topochemical Transformation of Phyllosilicate Clay into Chlorite and Brucite. Chemistry of Materials, 2004, 16, 3206-3208.	6.7	6
344	Electrophoretic Route to Bi2Sr2CaCu2O8+y Films and Microfibers from Superconducting Colloids. Advanced Materials, 2005, 17, 1742-1745.	21.0	6
345	Trivalent Atom Contribution on Solidâ Solid Transformation of Ga13Polycation Intercalated Clay into Sodalite Investigated by X-ray Absorption Spectroscopy. Journal of Physical Chemistry B, 2005, 109, 9432-9436.	2.6	6
346	Sepiocite, Sepiolite-Like Nanoclay Derived from Hydrotalcite-Like Layered Double Hydroxide. Journal of Nanoscience and Nanotechnology, 2011, 11, 382-385.	0.9	6
347	Y(III) ion substituted 2D anionic clay (I); in-vitro cytotoxicity and intercellular uptake behavior. Applied Clay Science, 2019, 176, 58-65.	5.2	6
348	Enhanced Contrast of Electrochromic Full Cell Systems with Nanocrystalline PEDOT-Prussian Blue. Journal of Nanoscience and Nanotechnology, 2007, 7, 4131-4134.	0.9	6
349	Intercalation of n-ankylmonoamine and n-alkyldiamine in VOC1. Materials Research Bulletin, 1985, 20, 1401-1408.	5.2	5
350	Electrochemically prepared high Tc superconductor, La2CuO4 + lf and its x-ray photoelectron spectroscopic analysis. Physica C: Superconductivity and Its Applications, 1991, 185-189, 567-568.	1.2	5
351	A New Method to Determine the Oxygen Content of YBa2Cu3O7\$-δ\$: Open-Circuit Voltage Measurement. Japanese Journal of Applied Physics, 1993, 32, L400-L402.	1.5	5
352	Crystal Structure and the Role of Covalency in Eight-Layered Hexagonal Ba2CrTaO6. Japanese Journal of Applied Physics, 1993, 32, 4628-4634.	1.5	5
353	Intercalation route to new superconducting and insulating hybrid systems, M–X–Bi2Sr2CanâÂ^Â'1 (M=Hg,Ag; X=Br,I; Py=pyridine; n=1,2). Solid State Ionics, 1998, 108, 17-22.	CunOy	5
354	X-ray absorption spectroscopic study on Bi2Sr2Ca1âÂ^Â'xYxCu2O8+δ (x=0–1). Solid State Ionics, 199 291-295.	98,108, 2.7	5
355	Transformation of Dion–Jacobson-type layered oxyfluorides into new anion-deficient pyrochlore-type oxides, ASrNb2O6.5 (A = Li and Na). Journal of Materials Chemistry, 2002, 12, 1001-1004.	6.7	5
356	Role of Iodine Species in Structural Stability of Nanocrystalline Manganese Oxyiodides. Electrochemical and Solid-State Letters, 2004, 7, A49.	2.2	5
357	A novel heterostructured RuS2–titanate nanohybrid. Journal of Physics and Chemistry of Solids, 2006, 67, 1248-1251.	4.0	5
358	Tailoring Porosity of Colloidal Boehmite Sol by Controlling Crystallite Size. Bulletin of the Korean Chemical Society, 2012, 33, 1962-1966.	1.9	5
359	NICLOSAMIDE-EXFOLIATED ANIONIC CLAY NANOHYBRID REPURPOSED AS AN ANTIVIRAL DRUG FOR TACKLING COVID-19; ORAL FORMULATION WITH TWEEN 60/EUDRAGIT S100. Clays and Clay Minerals, 2021, , 1-14.	1.3	5
360	Preparation and properties of new nickel bisdithiolene conductors, [n-Bu4N]0.29[Ni(dmbit)2] and [n-Bu4N]0.59[Ni(dmbbip)2]. Synthetic Metals, 1993, 56, 1705-1710.	3.9	4

#	Article	IF	CITATIONS
361	Stabilization of Unusual Oxidation States of Chromium, Cr(IV) and Cr(V), in the Ordered Perovskite La2LiV1-xCrxO6. Journal of Solid State Chemistry, 1994, 109, 289-294.	2.9	4
362	Magnetic properties of nickel(III) bis(benzene-1,2-dithiolate); (n-Bu4N)[Ni(dmbit)2] and (n-Bu4N)[Ni(dmbbip)2]. Synthetic Metals, 1995, 70, 1059-1060.	3.9	4
363	Evolution of high Tc superconductivity of Bi4Sr3â^'xLaxCa3Cu4Oy upon iodine intercalation. Synthetic Metals, 1995, 71, 1589-1590.	3.9	4
364	X-ray absorption spectroscopic (XAS) study of nickel bisdithiolenes, (n-Bu4N)x[Ni(dmbit)2] (x = 2, 1,) Tj ETQq0 0	0 rgBT /O [.] 2.2	verlock 10 Tf
365	XAFS Study on Cu(II) Complexes Stabilized in Two-dimensional Silicate Lattice, Hectorite. Molecular Crystals and Liquid Crystals, 1998, 311, 303-308.	0.3	4
366	Chemical bonding between host and guest in the(HgBr2)0.5Bi2Sr1.5â^'xLaxCa1.5Cu2Oy(x=0.0,0.2, and 0.4) superconducting-insulating nanocomposite system. Physical Review B, 1998, 57, 3156-3163.	3.2	4
367	Pure tetravalent nickel in \hat{I}^3 -type nickel oxyhydroxide as secondary battery electrode. Journal of Materials Research, 1998, 13, 880-882.	2.6	4
368	Anomalous Thermoelectric Power Behaviors of Iodine Intercalated (Bi,Pb)2Sr2Canâ^'1CunO2n+4+δSuperconductors (n=2 and 3). Journal of Solid State Chemistry, 1999, 142, 199-205.	2.9	4
369	Study of anomalous microstructure changes in Mn-doped Bi2201 system. Physica C: Superconductivity and Its Applications, 2005, 419, 85-93.	1.2	4
370	UV Screening of Ferulic Acid–Zinc Basic Salt Nanohybrid with Controlled Release Rate. Journal of Nanoscience and Nanotechnology, 2011, 11, 413-416.	0.9	4
371	Amorphous Tungstate Precursor Route to Nanostructured Tungsten Oxide Film with Electrochromic Property. Journal of Nanoscience and Nanotechnology, 2011, 11, 6518-6522.	0.9	4
372	Fabrication of pore window in ordered mesoporous silica by spatial control of functional groups. Chemical Engineering Journal, 2014, 253, 1-7.	12.7	4
373	Thermotropic phase transitions in the bidimensional compound (C10H21NH3)2Cucl4. Journal De Chimie Physique Et De Physico-Chimie Biologique, 1993, 90, 1829-1854.	0.2	4

374	Molecular Orientation of Intercalants Stabilized in the Interlayer Space of Layered Ceramics: 1-D Electron Density Simulation. Journal of the Korean Ceramic Society, 2016, 53, 417-428.	2.3	4
375	Preparation of the ordered perovskite (SrLa)(MgMo)O6 and its physico-chemical characterization. Journal of the Chemical Society Dalton Transactions, 1989, , 2335.	1.1	3
376	Synthesis and structural analysis of the new layered compound [FeWO4Cl]. Journal of the Chemical Society Dalton Transactions, 1991, , 1647.	1.1	3
377	Synthesis and magnetic properties of conductive nickel-dmbit complex. Synthetic Metals, 1995, 70, 1057-1058.	3.9	3

378 Correlation between Structure and Ionic Conductivity in Layered Perovskite Oxides, LiLnTa2O7 (LnËŁa,) Tj ETQq0 0.0 rgBT /Oyerlock 10

#	Article	IF	CITATIONS
379	Development of Electrochromic Devices Working with Hydrophobic Lithium Electrolyte. Active and Passive Electronic Components, 1998, 20, 201-213.	0.3	3
380	Tunneling characteristics of I- and HgI2-intercalated Bi2Sr2CaCu2O8+x single crystals. Physica B: Condensed Matter, 2000, 284-288, 1844-1845.	2.7	3
381	Chimie douce route to hetero-structured high-Tc cuprates. Solid State Sciences, 2001, 3, 253-263.	0.7	3
382	Origin of the Metallization ofc-Axis Resistivity upon lodine Intercalation into Bi2Sr2CaCu2O8+δ. Journal of Physical Chemistry B, 2001, 105, 5174-5177.	2.6	3
383	Polarized X-Ray Absorption Spectroscopic Study on Mercuric Bromide Intercalated Bi2Sr2CaCu2Oy Single Crystal. Journal of Solid State Chemistry, 2001, 160, 39-44.	2.9	3
384	Effect of Copper Doping on the Crystal Structure and Morphology of 1D Nanostructured Manganese Oxides. Journal of Nanoscience and Nanotechnology, 2007, 7, 4029-4032.	0.9	3
385	Diffusion Control of Porous Membrane by Modifying the Nanopore Properties. Journal of Nanoscience and Nanotechnology, 2011, 11, 1656-1659.	0.9	3
386	Surface Passivation of CeO ₂ Catalyst and Its Ultraviolet Screening Effect. Journal of Nanoscience and Nanotechnology, 2011, 11, 6448-6452.	0.9	3
387	Mesoporous Gallosilicate with 3 D Architecture as a Robust Energyâ€Efficient Heterogeneous Catalyst for Diphenylmethane Production. ChemCatChem, 2013, 5, 1863-1870.	3.7	3
388	Gene and Drug Delivery System with Soluble Inorganic Carriers. , 2008, , 349-367.		3
389	Hydrophobic Guest Mediated Micellization and Demicellization of Rationally Designed Amphiphilic Poly(organophosphazene) for Efficient Drug Delivery. Science of Advanced Materials, 2016, 8, 1553-1562.	0.7	3
390	A new 2-dimensional magnetic model for the layered compounds of FeMO4Cl(M=Mo and W) with strong interlayer coupling. Synthetic Metals, 1995, 71, 2055-2056.	3.9	2
391	XANES study and rietveld refinement for the nanometer sized polycrystalline ferrite, AFe12O19 (A=Sr,) Tj ETQq1	1	4 _{.2} gBT /Ove
392	X-Ray Absorption Spectroscopic Studies on Layered FeWO4Cl and Its Lithium Intercalate. Japanese Journal of Applied Physics, 1997, 36, 5605-5609.	1.5	2
393	Intracrystalline Structure of Chromium Oxide-Cluster Pillar in Montmorillonite. Molecular Crystals and Liquid Crystals, 1998, 311, 315-320.	0.3	2
394	Evolution of crystal and electronic structures of Sr2CuO3 upon fluorination reaction. Physica C: Superconductivity and Its Applications, 1999, 322, 93-99.	1.2	2
395	Intercalation Route to Novel Superconducting Nano-Hybrids. Molecular Crystals and Liquid Crystals, 2000, 341, 479-484.	0.3	2
396	OKand CuLIIIedge study of itinerant holes in I2-, HgI2- and HgBr2-intercalated BSCCO(2212) single crystals. Journal of Synchrotron Radiation, 2001, 8, 818-820.	2.4	2

#	Article	IF	CITATIONS
397	Dynamics of microwave-induced fluxons in Hgl2-intercalated Bi2Sr2CaCu2O8+l̂´ Josephson stacks. Physica C: Superconductivity and Its Applications, 2001, 362, 97-101.	1.2	2
398	Influence of Host Lattice on the Chemical Bonding Nature of Guest Species in High-Tc Superconducting lâ^'Bi2Sr1.5-xLaxCa1.5Cu2Oy Nanohybrids. Journal of Physical Chemistry B, 2004, 108, 12044-12048.	2.6	2
399	Novel synthesis of Bis (N-oxopyridine-2-thionato) zinc (II) using solid precursors. Journal of Physics and Chemistry of Solids, 2006, 67, 1071-1074.	4.0	2
400	Topographical Functionalization of Ordered Mesoporous Silica. Solid State Phenomena, 2006, 111, 139-142.	0.3	2
401	Soft-Chemical Synthesis and Electrochemical Characterization of Multicomponent Mn _{1–<i>x</i>–<i>y</i>} Co _{<i>x</i>} Ni _{<i>y</i>} O ₂ Nanostructures. Journal of Nanoscience and Nanotechnology, 2007, 7, 3857-3861.	0.9	2
402	A layer-by-layer assembly route to [Mn1/3Co1/3Ni1/3]O2 hollow spheres with electrochemical activity. Journal of Physics and Chemistry of Solids, 2012, 73, 1492-1495.	4.0	2
403	Titania Nanoparticles Stabilized HPA in SBA-15 for the Intermolecular Hydroamination of Activated Olefins. ChemCatChem, 2014, 6, 3267-3267.	3.7	2
404	Removal of Cyanobacteria <i>Anabaena flos-aquae</i> Through Montmorillonite Clays. Energy and Environment Focus, 2014, 3, 60-63.	0.3	2
405	X-ray Photoelectron Spectroscopic Evidence for Cu3+Valence State in Superconducting Phase, YBa2Cu3O7-δ. Molecular Crystals and Liquid Crystals Incorporating Nonlinear Optics, 1990, 184, 61-67.	0.3	1
406	Oxygen distribution in silver sheated YBa2Cu3O7â َ (َ/Ag0.3 superconducting wire determined by micro-Raman spectroscopy. Physica C: Superconductivity and Its Applications, 1991, 185-189, 2405-2406.	1.2	1
407	Thermodynamic studies on YBa2Cu3O7â^Î^ and Y2BaCuO5 by solution calorimetry. Materials Letters, 1992, 15, 156-161.	2.6	1
408	The Effect of Lithium Intercalation on the Crystal Structure and Magnetic Property of LayeredFeWO4Cl. Japanese Journal of Applied Physics, 1997, 36, 2656-2660.	1.5	1
409	X-RAY ABSORPTION SPECTROSCOPIC STUDIES AT THE ARSENIC K-EDGE FOR NEW TERNARY Li2S–B2S3–As2 GLASS SYSTEMS. Journal of Physics and Chemistry of Solids, 1998, 59, 1579-1584.	2S3 4.0	1
410	Metallization and 250 K anomaly of -intercalated Bi-2212 single crystals. Superconductor Science and Technology, 1998, 11, 133-137.	3.5	1
411	Polarization-dependent XANES study of Bi2Sr2Ca1-xPrxCu2O8-Î însulating single crystal. Journal of Synchrotron Radiation, 2001, 8, 842-844.	2.4	1
412	Conductive Polymer/Transition Metal Oxide Hybrid Materials for Lithium Batteries. Materials Research Society Symposia Proceedings, 2002, 726, 1.	0.1	1
413	Chemical synthesis and magnetic properties of a heterostructured spin system with superconducting and Pauli-type paramagnetic subsystems. Superconductor Science and Technology, 2005, 18, 470-476.	3.5	1
414	Time-Dependent X-ray Absorption Spectroscopic (XAS) Study on the Transformation of Zinc Basic Salt into Bis(N-oxopyridine-2-thionato) Zinc (II). Journal of Nanoscience and Nanotechnology, 2007, 7, 3867-3871.	0.9	1

#	Article	IF	CITATIONS
415	Mixed Micelle-Template Route to Mesoporous Silica. Journal of Nanoscience and Nanotechnology, 2007, 7, 3819-3822.	0.9	1
416	A room temperature etching route to tungsten oxide hydrate nanoplates with expanded surface area. Materials Letters, 2008, 62, 2297-2300.	2.6	1
417	Porous Organo-Functionalized Silica/Clay Hybrids. Journal of Nanoscience and Nanotechnology, 2008, 8, 5293-5296.	0.9	1
418	Facile Exfoliation of Layered Titanoniobate (KTiNbO5) into Colloidal Nanosheets. Journal of Nanoscience and Nanotechnology, 2009, 9, 7190-4.	0.9	1
419	Diffusivity control in nanoporous membrane through organic–inorganic hybridization. Journal of Physics and Chemistry of Solids, 2010, 71, 681-684.	4.0	1
420	Titania-pillared molybdenum oxide as a new nanoporous photocatalyst. Journal of Physics and Chemistry of Solids, 2012, 73, 1469-1472.	4.0	1
421	Highly Magnetic Nanoporous Carbon/Ironâ€Oxide Hybrid Materials. ChemPhysChem, 2014, 15, 3440-3443.	2.1	1
422	Enhanced contrast of electrochromic full cell systems with nanocrystalline PEDOT-prussian blue. Journal of Nanoscience and Nanotechnology, 2007, 7, 4131-4.	0.9	1
423	Characterization of 2:1 type layered aluminosilicate via intercalation reaction. Korean Journal of Chemical Engineering, 1984, 1, 99-104.	2.7	0
424	A solution calorimetric study on stability of superconducting YBa2Cu3O6.91. Physica C: Superconductivity and Its Applications, 1991, 185-189, 773-774.	1.2	0
425	An enhancement of electron localization in (Cuî—,O) bond upon vanadium substitution in YBa2Cu3â^'xVxO7â^'l´ superconductor. Physica C: Superconductivity and Its Applications, 1991, 185-189, 955-956.	1.2	0
426	A novel method to prepare highly dense ceramics of YBa2Cu3O7â^'σ. Physica C: Superconductivity and Its Applications, 1991, 185-189, 433-434.	1.2	0
427	Variation of covalent character of (Mn-O) bond in CaLaMgMnO6-xprepared under oxygen pressure of 60 kbar and 1 bar. High Pressure Research, 1991, 7, 293-295.	1.2	0
428	Structural and magnetic transformation of La/sub 2-x/Bi/sub x/CuO/sub 4/ induced by electrochemical oxidation. , 1994, , .		0
429	N-alkylammonium intercalated 2-D potassium titanates and their thermotropic phase transition. , 1994, , , \cdot		0
430	A new 2-dimensional magnetic model for the layered compounds, of FeMO/sub 4/CI(M=Mo and W) with strong interlayer coupling. , 1994, , .		0
431	Structural and magnetic transformation of La2â~'xBixCuO4 induced by electrochemical oxidation. Synthetic Metals, 1995, 71, 1627-1628.	3.9	0
432	Variation of (Mn-O) covalency in ALaMgMnO6-x(A = Ca, Sr, Ba) prepared under high pressure of 60kbar. High Pressure Research, 1995, 13, 183-192.	1.2	0

#	Article	IF	CITATIONS
433	<title>X-ray absorption spectroscopic study of new high-Tc superconducting intercalation compound
of
(HgX<formula><inf><roman>2</roman></inf></formula>)<formula><inf><roman>0.5</roman></inf></formula
(X=Br,I)</title> 1996,	a>Bi <form< td=""><td>ula><inf><roi< td=""></roi<></inf></td></form<>	ula> <inf><roi< td=""></roi<></inf>
434	Intercalation Route to New Hybrid Organic-Inorganic Superconductors. Molecular Crystals and Liquid Crystals, 1998, 310, 205-210.	0.3	0
435	Intercalation Route to New Hybrid Organic-Inorganic Superconductors. Molecular Crystals and Liquid Crystals, 1998, 311, 383-388.	0.3	Ο
436	New Mixed Conductors, Ag x I w Bi2Sr2Can-1CuaOy (0.75 < x < 1.2, n = 1, 2, and 3). Molecular Crystals and Liquid Crystals, 1998, 311, 423-428.	0.3	0
437	Novel Synthetic Route to Superconducting-Insulating Nanohybrids. Molecular Crystals and Liquid Crystals, 2000, 349, 323-328.	0.3	Ο
438	Intercalative Route to Heterostructured Nanohybirds. Materials Research Society Symposia Proceedings, 2001, 703, 1.	0.1	0
439	Insertion of Inorganic-Biomolecular Nanohybrid into Eucaryotic Cell. Materials Research Society Symposia Proceedings, 2001, 703, 1.	0.1	Ο
440	Local structure analysis of Ti species stabilized in ion exchangeable layer solids by X-ray absorption spectroscopy. Journal of Synchrotron Radiation, 2001, 8, 728-730.	2.4	0
441	A Novel Nanoparticle/Lamellar Oxide Hybrid: TiO2-pillared MoO3. Materials Research Society Symposia Proceedings, 2002, 755, 1.	0.1	0
442	Ferrimagnetic Membranes for Separation of Paramagnetic and Diamagnetic Species. Materials Research Society Symposia Proceedings, 2002, 752, 1.	0.1	0
443	Quantum-well structured high-Tc superconductors prepared by soft-chemical method. Current Applied Physics, 2003, 3, 401-403.	2.4	0
444	Topochemical Transformation of Phyllosilicate Clay into Chlorite and Brucite ChemInform, 2004, 35, no.	0.0	0
445	An Inorganic Nanohybrid with High Specific Surface Area: TiO2-Pillared MoS2 ChemInform, 2005, 36, no.	0.0	Ο
446	2P574 Bio-organic-inorganic ternary nanohybrids for DNA-barcode system(53. Bioengineering,Poster) Tj ETQq0	0 0 ₀ gBT /(Overlock 10 T
447	Hole states of X-Bi2Sr2CaCu2O8 [X=I, Hgl2, and (Py-CH3)2Hgl4] probed by O K-edge X-ray absorption spectroscopy. Journal of Physics and Chemistry of Solids, 2006, 67, 223-226.	4.0	0
448	FeWO4Cl as cathode material for lithium rechargeable battery. Journal of Electroceramics, 2009, 23, 305-311.	2.0	0
449	Inside Cover: A Dual-Polymer Electrochromic Device with High Coloration Efficiency and Fast Response Time: Poly(3,4-(1,4-butylene-(2-ene)dioxy)thiophene)-Polyaniline ECD (Chem. Asian J. 8/2011). Chemistry - an Asian Journal, 2011, 6, 1898-1898.	3.3	0
	Intercolative Ion Evoluting Doute to Aming Acid Lovered Double Hydrovide Nanobybride and Their		

450Intercalative Ion-Exchange Route to Amino Acid Layered Double Hydroxide Nanohybrids and Their
Sorption Properties. European Journal of Inorganic Chemistry, 2015, 2015, 898-898.2.00

#	Article	IF	CITATIONS
451	Rücktitelbild: Biodegradable Inorganic Nanovector: Passive versus Active Tumor Targeting in siRNA Transportation (Angew. Chem. 14/2016). Angewandte Chemie, 2016, 128, 4688-4688.	2.0	0
452	Nanoengineering Route to Two-Dimensional Hybrid Materials. , 2004, , 197-216.		0
453	Nano-engineering via intercalation: layer-by-layer interstratification of high-T c superconducting and superionic materials Ag x I y Bi 2 Sr 2 Ca n-1 Cu n O 2n+4 (n=1, 2, and 3). , 1996, , .		Ο